Synthetic and Systems Biotechnology 10 (2025) 794–806

Contents lists available at ScienceDirect

Synthetic and Systems Biotechnology

journal homepage: www.keaipublishing.com/en/journals/synthetic-and-systems-biotechnology

Original Research Article

A new paradigm for the regulation of A40926B0 biosynthesis

Yan-Qiu Liu [a,b], Yi-Lei Zheng [a,b], Ye Xu [a,b], Xue-Yan Liu [a,b], Tian-Yu Xia [a,b], Qing-Wei Zhao [a], Yong-Quan Li [a,b,*]

[a] First Affiliated Hospital and Institute of Pharmaceutical Biotechnology, Zhejiang University School of Medicine, Hangzhou, 310058, China
[b] Zhejiang Provincial Key Laboratory of Synthetic Biotechnology for Microbial Medicine, Hangzhou, 310058, China

ARTICLE INFO

Keywords:
A40926B0
Dalbavancin
Regulatory networks
WblA
Dbv3
GlnR
BkdR

ABSTRACT

Dalbavancin is a novel glycopeptide antibiotic with activity against a broad range of Gram-positive bacteria, including methicillin-resistant *Staphylococcus aureus* (MRSA). A40926B0 is the direct precursor of dalbavancin, but the regulatory mechanisms underlying its biosynthesis are not well understood. Additionally, the presence of seven homologs leads to significant metabolic burden, affecting both production and purity of A40926B0. To further reveal the transcriptional regulatory mechanism of A40926B0 biosynthesis in *N. gerenzanensis* L70, this study employed multiple strategies to explore the regulatory network of its biosynthesis from both intracluster and extracluster aspects. WblA regulates gene expression within and outside the biosynthetic gene cluster (BGC), impacting multiple biosynthetic pathways, and Dbv3, a key regulator in the A40926B0 cluster, positively influences biosynthesis. Using a bottom-up (DNA to protein) regulator mining strategy with the key intra-cluster regulator Dbv3, it was determined that GlnR is also involved in the regulation of secondary metabolism, while BkdR regulates precursor supply. By constructing the combination of GlnR, BkdR and Dbv3 together with the WblA deletion, the regulatory network of A40926B0 was reconstructed, resulting in a 92 % improvement in purity of A40926B0. The objective of this study is to elucidate the regulatory mechanisms governing A40926B0 biosynthesis by constructing a comprehensive, multidimensional model of its regulatory network. The findings of this study serve to enhance our comprehension of A40926B0 biosynthesis and furnish insights into broader strategies for enhancing the production of other natural products and secondary metabolites in industrial microbiology.

1. Introduction

Dalbavancin, a novel glycopeptide antibiotic, exhibits activity against a broad spectrum of Gram-positive bacteria, including methicillin-resistant *Staphylococcus aureus* (MRSA), and partially binds the heptapeptide backbone to the d-alanyl-D-alanine (d-Ala-d-Ala) terminus of the growing peptidoglycan chain, inhibiting bacterial cell wall synthesis [1–5]. As a novel antibiotic against multidrug-resistant bacteria, dalbavancin has significant commercial potential. Its early clinical development focused on a once-weekly infusion regimen (1000 mg on day 0 and 500 mg on day 7) for treating acute bacterial skin and skin structure infections (ABSSSIs), leading to its approval by the U.S. Food and Drug Administration (FDA) in 2014 [3,6–9].

Dalbavancin is derived from the natural glycopeptide A40926 [10], a mixture of compounds featuring different fatty acyl side chains. According to the FDA approval guidelines for dalbavancin, which is composed of A0, A1, B0, B1 and B2, the B0 component, which contains an isododecanol side chain, accounts for over 75 % of the complex [11,12]. A40926B0 undergoes esterification of the carboxyl group on aminoglucuronic acid, amidation of the carboxyl group at position 38, followed by hydrolysis of the ester in an alkaline solution, acidification, and salt formation, ultimately yielding dalbavancin [13]. Fermentation of *Nonomuraea gerenzanensis* L70, a strain that produces the dalbavancin precursor A40926B0, results in the production of A40926B0 together with seven homologous congeners. These congeners consist of molecules with straight or branched chain fatty acyl groups containing 11 to 14 carbon atoms. In addition, the high proportion of seven homologs would cause a significant metabolic burden, affecting the production and

Peer review under the responsibility of Editorial Board of Synthetic and Systems Biotechnology.
* Corresponding author. First Affiliated Hospital and Institute of Pharmaceutical Biotechnology, Zhejiang University School of Medicine, Hangzhou, 310058, China.
E-mail address: lyq@zju.edu.cn (Y.-Q. Li).

https://doi.org/10.1016/j.synbio.2025.03.012
Received 7 January 2025; Received in revised form 27 March 2025; Accepted 31 March 2025
Available online 7 April 2025

purity of A40926B0, resulting in a purity of A40926B0 of less than 30 %, making it difficult to realise its medicinal value [14–18].

The efficiency of microbial drug biosynthesis is often influenced by regulatory networks as well as key synthetic enzymes [19,20]. Advancements in the study of regulatory mechanisms governing antibiotic biosynthesis in actinomycetes have led to the development of various tools to reconstruct known regulatory pathways. These strategies include overexpression of positive regulators, silencing of repressors, and ribosome engineering [21]. The successful implementation of these approaches has not only improved the production of secondary metabolites but also advanced our understanding of the regulatory mechanisms involved [22]. Numerous pleiotropic regulators have been shown to influence the biosynthesis of secondary metabolites. For example, MtrA regulates the production of chloramphenicol and jadomycin in *Streptomyces venezuelae* [23] and fidaxomicin in *Actinoplanes deccanensis* YP-1 [24]. Similarly, AtrA is essential for morphogenesis and secondary metabolism in *Streptomyces roseosporus* [25], while in *Streptomyces griseus*, AtrA cooperates with AdpA to bind the *strR* promoter, where it conditionally regulates streptomycin production while negatively affecting avermectin biosynthesis [26]. These pleiotropic and pathway-specific regulators form an interconnected regulatory network, and remodeling this network can significantly boost secondary metabolite production [27].

As for A40926B0, the biosynthetic gene cluster contains two pathway-specific regulators (*dbv3* and *dbv4*) and a pair of genes involved in a two-component regulatory system (*dbv6* and *dbv22*) [28]. Transcript levels of *dbv3*, *dbv4*, *dbv5*, *dbv23* and *dbv24* were increased approximately 2- to 5-fold in *Δdbv6* and 5- to 20-fold in *Δdbv22*. Dbv6 was able to bind directly to the upstream region of the target genes, resulting in increased antibiotic production, suggesting that Dbv6 and Dbv22 negatively regulate the production of A40926 [29]. Dbv4 regulates biosynthesis by binding to the upstream regions of *dbv14* and *dbv30*, leading to enhanced transcription of the *dbv8-14* and *dbv30-35* operons and increased antibiotic production. In contrast, the regulatory target of Dbv3 was only predicted by qRT-PCR analysis of the transcript levels of each gene. The results clearly showed that *dbv1*, *dbv4*, *dbv14*, *dbv15*, *dbv20*, *dbv29* and *dbv32* are either not transcribed or are transcribed 10-fold less in the *Δdbv3* strain than in the parental strain, but there is no evidence to date for a direct regulatory target of Dbv3 [30]. Identifying the binding sites of Dbv3 within the gene cluster will provide further insights into its regulatory mechanism.

The aim of this study was to elucidate the regulatory mechanisms governing the biosynthesis of A40926B0, the direct precursor of the novel antibiotic dalbavancin, and to improve its production and purity. The role of the pleiotropic regulator WblA in modulating genes both within and outside the biosynthetic gene cluster was investigated. For the first time, the pathway-specific regulatory role of Dbv3 in A40926B0 biosynthesis was identified, revealing a cascade regulatory pattern involving Dbv3 and Dbv4 within the gene cluster. These findings provide a basis for further investigation into the regulatory network governing A40926B0 biosynthesis. GlnR, a global transcriptional regulator of nitrogen metabolism, was identified from the *N. gerenzanensis* L70 proteome using a 5′-biotin-labeled P2 (upstream region of *dbv3*) probe. The regulatory mechanism of BkdR, a key factor in precursor biosynthesis, was also explored. By integrating both intra- and extra-cluster regulatory pathways, a three-dimensional model of the A40926B0 biosynthetic network is proposed, encompassing precursor supply regulation, pleiotropic regulation, and pathway-specific regulation.

2. Materials and methods

2.1. Strains, plasmids, primers, and culture methods

All strains and plasmids used in this study are listed in Table S1, and all primers are provided in Table S2.

Escherichia coli was cultured at 37 °C in liquid Luria-Bertani (LB) medium, composed of 1 % peptone, 0.5 % yeast extract, and 1 % sodium chloride (2 % agar should be added to the solid medium), with 1 % of corresponding antibiotics.

N. gerenzanensis L70 and its derived mutant strains were cultured on YMG solid medium (0.4 % glucose, 0.4 % yeast extract, 1 % malt extract, 0.2 % calcium carbonate, 2 % agar, pH 7.3) at 28 °C, supplemented with 1 % corresponding antibiotics (final concentration: 50 μg/mL).

For fermentation, strong growing mycelia were picked in YMG solid medium and transferred to 100 mL flasks containing 20 mL of seed medium YEME (0.5 % peptone, 0.3 % yeast extract, 0.3 % malt extract, 4 % dextrose) and incubated at 28 °C, 220 rpm for 3 days. Thereafter, the seed culture was transferred into a 250 mL flask containing 35 mL of the fermentation medium YS (0.8 % soluble starch, 0.3 % malt extract, 0.2 % yeast extract, pH 9.5), at a 2 % inoculum, and the flask was then subjected to fermentation for a period of 7 days under the same conditions (28 °C, 220 rpm). Each fermentation batch was repeated three times and each time each strain had three parallel.

For the conjugation of *N. gerenzanensis* L70 and *E. coli* ET12567/pUZ8002, MS solid medium (2 % mannitol, 2 % cooked soybean meal, 2 % agar, 30 mM magnesium chloride) and 2 × YT liquid medium (1.6 % peptone, 1 % yeast extract, 0.5 % sodium chloride) were used.

2.2. Knockout and overexpression strain construction method

Fragments were amplified using KOD FX polymerase (Yeasen, Shanghai, China) and the corresponding primers (F + R). The linearized vector was digested with the appropriate restriction enzymes (Waltham, MA, USA). The amplified fragments were then ligated into the linearized vectors using the ClonExpress MultiS One Step Cloning Kit (Vazyme, Nanjing, China). The resulting constructs were transferred into *E. coli* DH5α cells, and correct clones were confirmed by sequencing.

For the construction of knockout vectors, the plasmid pSET153 was used, which contains 3-kb homology arms flanking the target gene. To generate overexpression vectors, the plasmid pIJ8660G was utilized, which contains the target gene under the control of a strong promoter, *ermE*p*. The vectors were then transferred into *E. coli* ET12567/pUZ8002 for conjugative transfer and introduced into *N. gerenzanensis* L70 by intergeneric conjugation.

Knockout strains were verified by PCR using a whole-frame knockout strategy with primers listed in Table S2. Overexpression strains were confirmed by PCR, using primers specific to the vector resistance gene and those listed in Table S2.

2.3. Transformation of N. gerenzanensis L70

Preparation of donor *E. coli*: The target plasmid was introduced into *E. coli* ET12567/pUZ8002 through transfer. Positive clones were selected and inoculated into 5 mL LB liquid medium supplemented with 1 % corresponding antibiotic for overnight incubation at 37 °C. Subsequently, 1 % (v/v) of the culture was transferred to 30 mL fresh LB medium containing 1 % corresponding antibiotic and incubated at 37 °C until reaching an OD_{600} of 0.4–0.6.

Preparation of receptor *N. gerenzanensis* L70: Vigorous mycelial fragments from *N. gerenzanensis* colonies grown on YMG solid medium were inoculated into 30 mL YEME liquid medium and cultured at 28 °C for 60–84 h 2 % (v/v) of the culture was then transferred into 35 mL YS liquid medium for a further 48 h incubation at 28 °C. Mycelial pellets were collected by centrifugation at 2800×*g* for 3 min before medium exchange.

Following the preparation of the donor and receptor, both were harvested by centrifugation (2800×*g*, 3 min). The bacterial pellets were processed separately: *E. coli* cells were washed three times with LB medium, while *N. gerenzanensis* mycelia received a single wash with 10 % glycerol solution. The washed pellets were combined and resuspended in 1 mL 2× YT medium. Following brief centrifugation (2800×*g*, 3 min), 500 μL supernatant was carefully removed. The remaining cell

mixture was thoroughly resuspended and plated on MS solid medium. Plates were initially incubated at 28 °C for 18 h before overlay supplementation with nalidixic acid (final concentration: 25 μg/mL) and plasmid-specific antibiotic (final concentration: 50 μg/mL). Subsequent incubation continued at 28 °C for 7–10 days to permit conjugant selection.

2.4. Dry weight experiment

The strains were initially cultivated in YEME medium for 3 days, after which they were transferred to YS fermentation medium. The initial growth status of each strain was standardized by adjusting the initial OD600 to 0.4. Samples were collected at 24, 48, 72, 96, 120, 144, and 168 h. After collection, the samples were centrifuged to remove the supernatant, and the pellets were dried at 65 °C for 3 days to ensure complete evaporation of the water. The dry weight was determined using an electronic balance, calculated as the difference in weight between the sample tube and the empty tube. Each experiment was performed in triplicate (n = 3).

2.5. HPLC analysis of A40926

Fermentation broths from *N. gerenzanensis* L70 and its mutant strains were collected after 7 days of YS fermentation. An equal volume of methanol was added to break the cells. The samples were collected by centrifugation and analyzed by HPLC (Agilent 1260 Infinity system, Agilent Technologies), as previously described. Pure A40926B0 (WeiShi Reagent, Wuhan, China) served as the standard, and the analysis was performed with UV detection at 220 nm.

2.6. Morphological observation of mutants

Morphological observations were conducted using the solid medium described above. *N. gerenzanensis* L70 and its mutant strains were cultured on YMG solid medium at 28 °C for 7 days, and their growth was recorded.

For scanning electron microscopy (SEM) analysis, samples were fixed in 0.1 M phosphate buffer (pH 7.4) containing 2.5 % glutaraldehyde for 8 h at 4 °C, followed by three washes with PBS. The samples were then post-fixed with 1 % OsO_4 for 2 h. After further washing with PBS to remove excess OsO_4, the samples underwent dehydration in ethanol gradients (30 %, 50 %, 70 %, 80 %, 90 %, and 100 %) for 15 min each. Finally, the samples were critical-point dried, coated, and examined using scanning electron microscopy. SEM analysis was performed by the ZJU Center for Cryo-Electron Microscopy (ZJU-CCEM).

2.7. Affinity isolation of P2-interacting proteins

To identify P2-interacting proteins, DNA affinity experiments were performed [25,31,32]. The P2 fragments were first cloned into the pTA2 vector. Biotin-labeled P2 probes were then synthesized by PCR using the primers pTA2-F and pTA2-R. The affinity isolation of the target proteins was carried out, and the samples were subjected to LC-MS/MS analysis to identify the interacting proteins.

2.8. Quantitative RT-PCR and RNA-seq analysis

To prepare genomic DNA-free RNA, RNA isolation was performed as follows. Samples were collected from 3 independent biological replicates of YS fermentation at 48 and 72 h. Mycelia were collected and washed twice with RNase-free TE buffer. Total RNA was then prepared from the mycelia using the EASYspin Plus bacteria RNA extract kit (Aidlab Biotech, Beijing, China). RNA samples were reverse transcribed into cDNA using the HiScript III 1st Strand cDNA Synthesis Kit (+gDNA wiper) (Vazyme, Nanjing, China) following the manufacturer's instructions.

To analyze transcription units in the A40926 biosynthesis gene cluster, the cDNA of *N. gerenzanensis* L70 was utilized as the template for reverse transcriptase PCR (RT-PCR) by rTaq polymerase with primer pairs (Table S2). qRT-PCR was performed as previously described [18], using the σ-factor gene *hrdB* as the internal control. Each primer pair was analyzed at least three times, with three parallels for each analysis.

For RNA-seq analysis, RNA was extracted from WT and *ΔwblA* strains, and libraries were constructed. All RNA samples were prepared as above from mycelia cultured for 48 and 72 h. A total of 3 lg RNA per sample was used as input material for transcriptome sequencing. The preparations were sequenced on an Illumina Novaseq platform (Illumina, San Diego, CA, USA) and 150 bp paired-end reads were generated. HTSeq v0.6.1 was used to count the number of reads mapped to each gene. Fragments per kilobase of transcript per million mapped reads (FPKM) were calculated to estimate gene expression levels. The transcriptomes were sequenced and analyzed by Azenta (Suzhou, China). The transcriptomic data have been deposited in the NCBI database.

2.9. Electrophoretic mobility shift assays (EMSA)

The target fragment was amplified using primers listed in Table S2 and cloned into the pET28a+6his vector to generate a recombinant plasmid for protein expression. After verifying the sequence, the plasmid was transferred into *E. coli* BL21 (DE3) cells, and positive clones were selected. The monoclonal strain was cultured in LB liquid medium at 37 °C until the OD_{600} reached 0.4–0.6. Protein expression was induced by adding 0.2 mM isopropyl-β-D-thiogalactopyranoside (IPTG), followed by incubation at 16 °C and 160 rpm for 16–18 h. The bacteria were harvested, and the soluble histidine-tagged proteins were purified using Ni-NTA resin. Bacteria were washed with pre-cooled Tris-HCl buffer and resuspended. Cells were disrupted by sonication in an ice-water mixture (sonication conditions: 30 % output power) and the supernatant was mixed with Ni-NTA resin after centrifugation. After 1 h of incubation, the incubation solution was filtered and the Ni-NTA was resuspended in Tris-HCl buffer and washed twice. This was followed by washing with 20 mM imidazole buffer to remove proteins that bind non-specifically to Ni-NTA. Finally, proteins were eluted with 250 mM imidazole buffer and the eluate was ultrafiltered and stored in 15 % glycerol. Protein concentration was determined and purity identified by SDS-PAGE. The purified proteins were stored at −80 °C.

To prepare the probes for EMSA, the specific target fragment was amplified using the primers in Table S2 and ligated into the pTA2 vector to obtain the recombinant vector. The promoter region of the target gene was then amplified from the recombinant vector template using pTA2-F (5′ FAM) and pTA2-R primers. The DNA concentration was measured using a micro-volume nucleic acid quantifier and stored at −20 °C.

For EMSA, the prepared probes were incubated with increasing concentrations of purified recombinant proteins at 30 °C for 30 min in a 10 μL reaction mixture. Each reaction contained 100 ng of probe, and the protein concentration was gradually increased. The specific experimental methods for EMSA were described previously [33].

2.10. GusA reporter analysis

A *gusA* (β-glucuronidase)-based reporter system was constructed to study promoter-protein interactions. The specific target fragment of the probe was amplified using primers listed in Table S2 and ligated into the pLRM02 vector to obtain a recombinant plasmid. The resulting pLRM02-Probe-*gusA* plasmid was used as the *gusA* reporter plasmid. This plasmid was then transferred into the knockout strain by conjugation and integrated into the genome. Specific methods of conjugative transformation are detailed in 2.3.

The strain was cultured in YEME medium for 72 h, after which mycelium was harvested for further analysis. Glucuronidase activity in the cell lysates was measured spectrophotometrically following a 2-h incubation at 37 °C. The protein concentration in the lysates was

determined using the Bradford assay to normalize for any differences between the samples.

3. Results

3.1. Function of WblA in N. gerenzanensis L70

WblA is recognized as a key transcriptional regulator involved in morphological differentiation and development [34]. A comparison of protein sequences revealed that ORF0351 in *N. gerenzanensis* L70 was homologous to WblA, sharing significant similarity with WblA proteins from other actinomycetes (Fig. S3A). Consequently, ORF0351 was designated as *wblA*. To investigate its function, both a knockout strain and overexpression strain of *wblA* were constructed. Phenotypic analysis on solid media showed that the *ΔwblA* strain exhibited impaired growth and failed to produce aerial mycelium (Fig. S1C). Additionally, the growth curve of *ΔwblA* in liquid medium was significantly lower than that of WT, indicating that the knockout of *wblA* inhibited the growth of the strain (Fig. 1A). It was shown that *N. gerenzanensis* L70 contains the *vpk* gene cluster, which encodes a violet pigment produced as a by-product of competition for precursors in the biosynthesis of A40926B0 [18]. Notably, increased violet pigment synthesis was observed in both solid and liquid cultures of *ΔwblA* (Fig. S1D). Scanning electron microscopy revealed that WT cells were elongated and branched, indicative of aerial mycelium, while *ΔwblA* cells were shorter and unbranched, suggesting a severe disruption in aerial mycelium formation (Fig. 1B). In contrast, the morphology of the overexpression strain was similar to that of WT (Fig. S2). Overall, these findings suggest that disruption of *wblA* significantly impairs cell growth, whereas overexpression of *wblA* promotes normal cell growth. Knockout of *wblA* increased the production of A40926B0 by 42 % to 188 mg/L, whereas overexpression reduced its biosynthesis by 20 % to only 105 mg/L (Fig. 1C). Similar trends were observed for other homologs [17,18], indicating that WblA negatively regulated both A40926 homologs and their byproduct, violet pigment (Fig. 1D).

To investigate the global regulatory effects of WblA in *N. gerenzanensis* L70, transcriptomic analysis was performed on WT and *ΔwblA* (Fig. S3). At 48 h, WblA was found to primarily regulate several primary metabolic pathways, particularly those involved in fatty acid metabolism (Fig. 1E). At 72 h, WblA's regulatory influence shifted towards amino acid metabolism and pathways related to secondary metabolite biosynthesis (Fig. 1F).

Transcriptomic data indicated that although *wblA* knockout resulted in a decrease in the expression of both key synthetic and regulatory genes in the A40926B0 biosynthetic gene cluster. Concurrently, however, the expression of other secondary metabolism-related genes changed significantly, leading to an increase in the production of A40926B0 (Figs. S4A–B). Moreover, knockout of *wblA* resulted in a marked increase in the transcript levels of genes involved in violet pigment biosynthesis, consistent with the observed phenotypic changes (Fig. S4C).

The regulatory mechanism of WblA was the subject of further investigation, building on previous morphological observations. The WblA protein was first expressed and 11 probes were designed based on the promoter regions of transcriptional units within the *dbv* gene cluster (P1–P11) (Figs. S5A–B). Local sequence alignment revealed that FtsK proteins, identified in the synthesized aerial mycelium, share significant similarity with WblA [35–38]. Among these, the promoter with the largest change in FPKM value, designated P*orf1243*, was selected as a probe (Fig. S3B). Additionally, the promoter of the key gene involved in the synthesis of the violet pigment byproduct, designated P*orf8714*, was also utilized as a probe (Fig. S3C).

Electrophoretic mobility shift assay (EMSA) experiments were conducted to assess potential interactions between the WblA protein and each of the FAM-tagged probes. However, no significant binding was observed between WblA and the promoter sequences. To date, no direct evidence has been found to support the binding of WblA to target promoter sequences, likely due to the structural characteristics of WblA [38,39]. To further investigate potential regulatory interactions, the *gusA* reporter system was employed. The results demonstrated that WblA directly regulated eight transcriptional units within the *dbv* gene cluster, including genes involved in regulators, NRPS synthesis, and modifications (Fig. 1H). Combining phenotypic and transcriptomic data, promoter regions where WblA is likely to exert regulatory effects were selected (Table S3). Using the *gusA* reporter system, interactions between WblA and these promoters were further examined, thereby revealing that WblA modulated genes coding for proteins involved in amino acid and fatty acid metabolism, which in turn affected A40926 biosynthesis (Fig. 1J).

Quantitative RT-PCR (qRT-PCR) analysis further confirmed that *wblA* knockout resulted in elevated transcript levels of regulators within the *dbv* gene cluster, while concurrently repressing the transcription of genes involved in amino acid biosynthesis (Fig. 1G). Moreover, *wblA* knockout significantly affected the transcript levels of genes associated with amino acid and fatty acid metabolism (Fig. 1I). In this subsection, we demonstrated that the transcriptional regulator *wblA* in *N. gerenzanensis* L70 had a dual role as a positive regulator of cell growth and a repressor of A40926B0 biosynthesis; transcriptome analyses further revealed that *wblA* negatively regulated fatty acid and amino acid metabolism while positively regulating genes involved in secondary metabolite biosynthesis.

3.2. Identification of Dbv3 binding sites in the A40926B0 biosynthetic gene cluster

In order to gain a deeper understanding of the cascade regulatory network of A40926B0 biosynthesis, the focus was shifted to the study of the regulatory mechanisms of pathway-specific regulators in the biosynthetic gene cluster. It has been shown that the *dbv* gene cluster includes four regulators, comprising the pathway-specific positive regulators *dbv3* and *dbv4*, as well as *dbv6* and *dbv22*, which form a two-component system involved in regulatory control [28–30]. Although there are no studies on the binding domain of Dbv3, our investigations have shown that *Δdbv3* strains promote aerial mycelial growth, yet neither the *Δdbv3* strain nor *dbv3* overexpression significantly affects the growth of wild-type (WT) strains (Fig. 2A and B). Notably, while overexpression of *dbv3* had no significant effect on the growth of the strain and promoted A40926B0 biosynthesis by only about 10 %, knockout of *dbv3* completely halted the production of all A40926 homologs, suggesting that Dbv3 is the most critical regulator for A40926B0 biosynthesis (Fig. 2C and D). Transcriptomic analysis further indicated a significant reduction in the expression of nearly all genes within the *dbv* cluster following *dbv3* knockout, while overexpression of *dbv3* led to a marked upregulation of other genes (Fig. 2F). These results highlight the crucial role of *dbv3* as a central regulator within the *dbv* cluster and emphasize the need for further exploration of its regulatory targets.

Dbv3 was identified as a member of the LuxR family, which function as pathway-specific regulators (Fig. S6A). To further investigate its binding characteristics, the DNA-binding domain (DBD) of Dbv3 was expressed, and EMSA experiments were conducted using 11 pre-constructed probes from the biosynthetic gene cluster (Figs. S6B–C). The Dbv3-DBD protein specifically bound to the P3 (upstream regions of *dbv4*) and P11 (upstream regions of *dbv36* and *dbv37*) probes, leading to gel retardation, while no significant binding was observed with the other nine probes (Fig. 2E). These results indicated that the binding site of Dbv3 was located in the upstream region of *dbv4* and *dbv36-37*, thus positively regulating the biosynthesis of A40926B0.

3.3. Identification of GlnR as a regulator of dbv3 promoter interaction by DNA affinity

Since *dbv3* is the most important pathway-specific regulator within

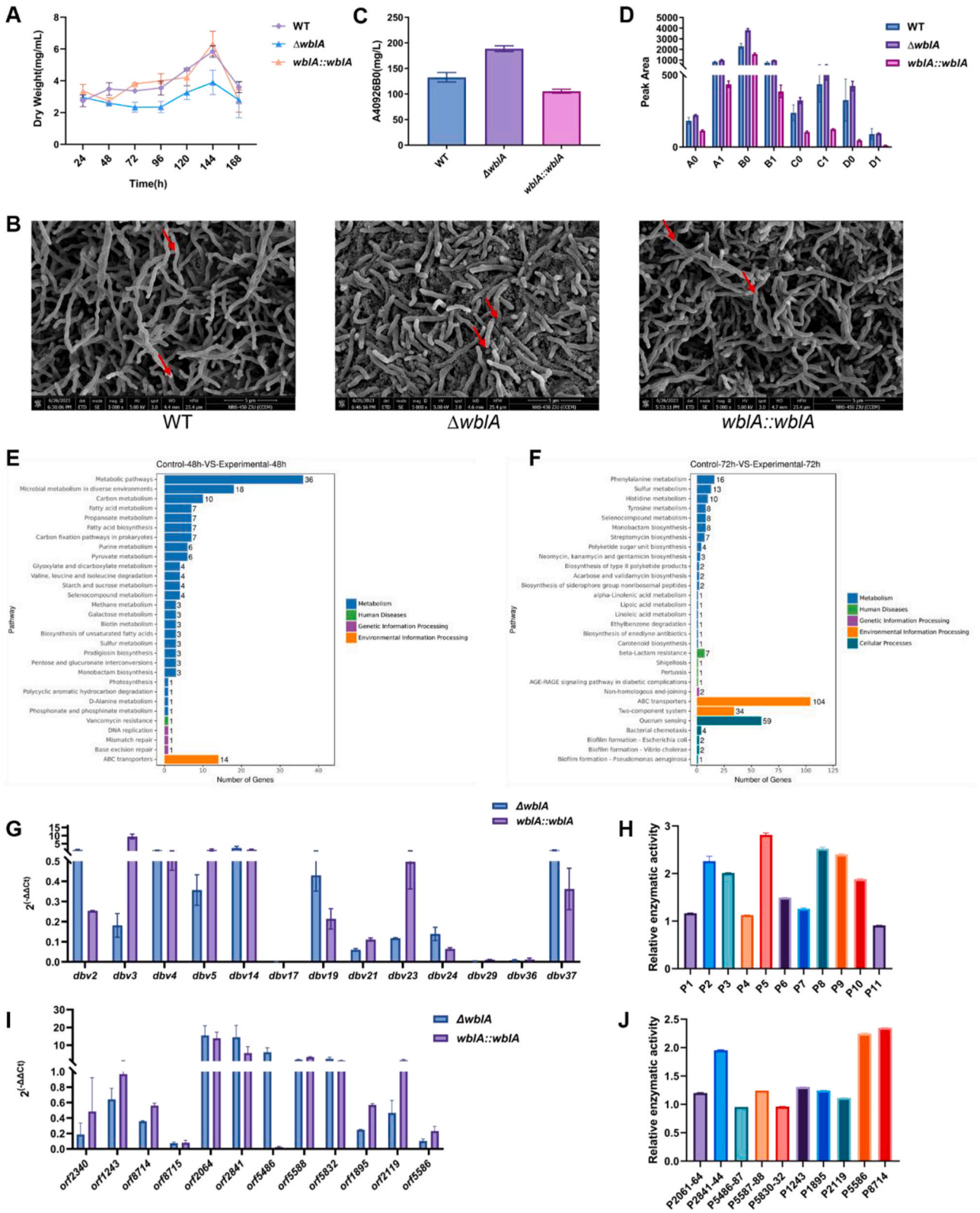

Fig. 1. Functional and regulatory mechanisms of WblA. (A) Effect of *wblA* deletion on cell growth. Fermentation in YS liquid medium. (n = 3, mean ± SD). (B) Effect of *wblA* deletion on cell morphology. White error bars represent a scale bar of 10 μM. (C) Effect of *wblA* deletion on A40926B0 production. (n = 3, mean ± SD). (D) Effect of *wblA* deletion on the production of each homolog of A40926B0. (n = 3, mean ± SD). (E–F) Differential gene enrichment statistics in KEGG pathways. The distribution statistics of differential gene enrichment in KEGG pathways in the WT and *ΔwblA* transcriptomes at 48 h (E) and 72 h (F). (G) Effect of *wblA* deletion on transcript levels of each transcriptional unit of the *dbv* cluster. (n = 3, mean ± SD). (H) Promoter assay for interaction with the WblA protein. (n = 3, mean ± SD). (I) Effect of *wblA* deletion on transcript levels of other transcriptional units of secondary metabolism. (n = 3, mean ± SD). (J) Promoter assay for interaction with the *wblA* protein in secondary metabolism. (n = 3, mean ± SD).

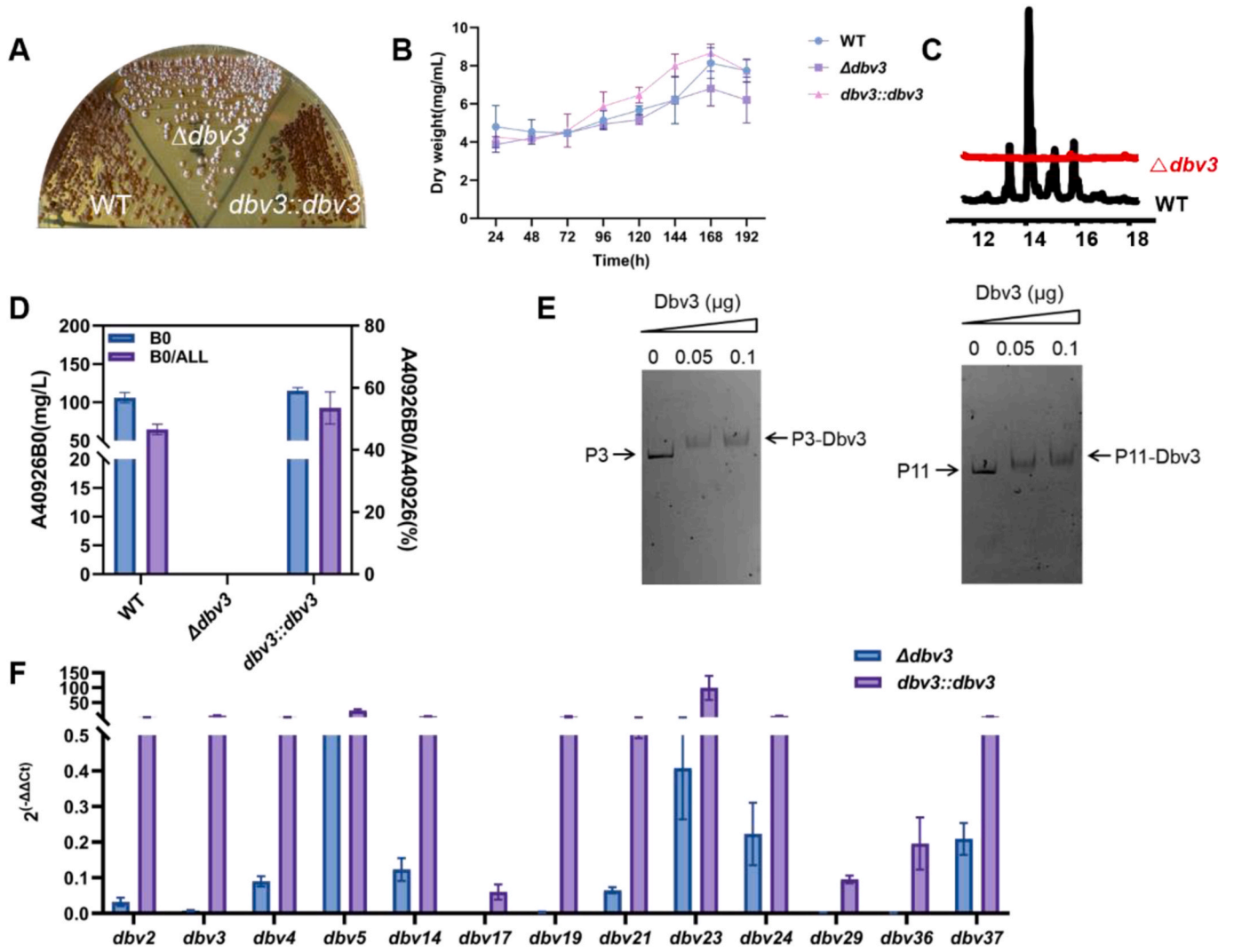

Fig. 2. Study of the regulatory mechanism of Dbv3. (A) Effect of *dbv3* deletion on cell growth on solid medium. (B) Effect of *dbv3* deletion on cell growth on liquid medium. (n = 3, mean ± SD). (C) HPLC analysis of the components of the *dbv3*-deficient fermentation extract A40926. (D) Effect of *dbv3* deletion on A40926B0 production. (n = 3, mean ± SD). (E) Binding site probing of Dbv3. Lanes from left to right represent experiments with increasing amounts (0 μg, 0.05 μg, and 0.1 μg) of purified Dbv3 protein binding to the probes. (F) Effect of *dbv3* deletion on the transcript levels of each transcriptional unit of the *dbv* cluster. (n = 3, mean ± SD).

the *dbv* BGC [30], in order to further investigate the transcriptional cascade regulating *dbv*3, a biotin-labeled DNA fragment of the *dbv*3 promoter (P2) was employed as bait to isolate potential regulators outside the A40926B0 BGC that may interact with P2 from WT mycelial lysates. The capture process is illustrated in the figure below (Fig. 3A). Liquid Chromatography-Tandem Mass Spectrometry (LC-MS/MS) analysis identified a total of 47 regulators. Based on their score and coverage, this study selected the top four candidates: *orf2314*, *orf3621*, *orf9722*, and *orf0768* (Table S4). These proteins were subsequently expressed and purified in *Escherichia coli* BL21 (DE3). The EMSA results demonstrated that only GlnR (encoded by *orf0768*) specifically bound to the P2 promoter (Fig. S7).

GlnR is a global transcriptional regulator of nitrogen metabolism in *Streptomyces coelicolor* [40]. Both knockout and overexpression strains of *glnR* were constructed. The growth of *ΔglnR* strain in liquid medium was enhanced compared to the WT, while growth on solid medium was comparable to that of WT. Overexpression of *glnR* led to increased violet pigment production (Fig. 3B and C). In terms of secondary metabolism, the biosynthesis of A40926B0 in the *ΔglnR* strain was reduced by 12 %, while overexpression of *glnR* resulted in a 20 % increase in the production of A40926B0 (Fig. 3D). Although the binding site remained unidentified, the above results suggested that GlnR was a positive regulator of A40926B0 biosynthesis.

Subsequently, the binding targets of GlnR were investigated using EMSA (Fig. S8). The results demonstrated that GlnR directly interacts with several regulators within the *dbv* cluster, including *dbv3*, *dbv4*, and *dbv22* (Fig. 3E). Notably, *orf1243*, associated with aerial mycelium growth and pigment synthesis, suggested that GlnR may directly regulated both A40926 biosynthesis and the production of aerial mycelium and pigments. Further EMSA analysis using pre-constructed WblA probes revealed that GlnR also interacts with proteins involved in amino acid and fatty acid metabolism (Fig. 4A).

qRT-PCR experiments confirmed that overexpression of GlnR significantly upregulated the transcription of genes within the *dbv* cluster (Fig. 4B), as well as those involved in amino acid and fatty acid metabolism (Fig. 4C). This upregulation correlated with enhanced biosynthesis of A40926B0. In this section, GlnR was bottom-up fished out from *dbv* BGC using a biotin-tagged P2 promoter and identified as a key positive regulator of A40926B0 biosynthesis, constituting a cascade regulatory pathway together with the intracluster positive regulator *dbv3*.

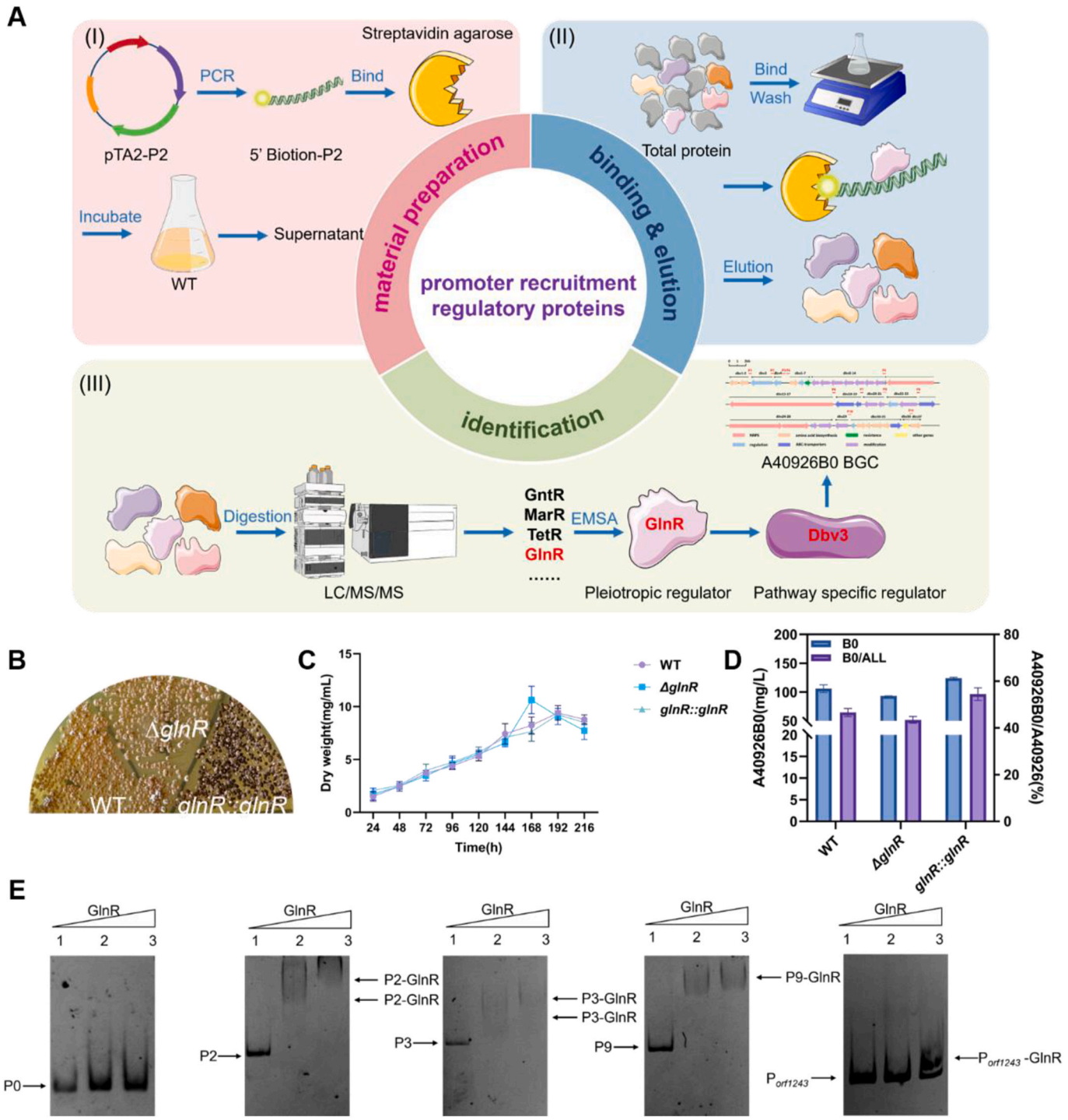

Fig. 3. Identification of GlnR, a regulator interacting with P2, and investigation of its regulatory mechanism. (A) Strategy for isolating proteins interacting with P2 from the *N. gerenzanensis* L70 proteome using an affinity-based approach. (B) Impact of *gln*R deletion on cell growth in solid medium. (C) Effect of *glnR* deletion on mycelial growth in liquid medium. (n = 3, mean ± SD). (D) Influence of *glnR* deletion on A40926B0 production. (n = 3, mean ± SD). (E) Binding site analysis of GlnR. EMSA showing GlnR binding to P2, P4, P9, and P*orf1243* probes. Lanes 1–3 show binding with 0 μg, 0.05 μg, and 0.1 μg of purified GlnR protein, respectively.

3.4. BkdR regulatory mechanisms involved in precursor supply

In addition to regulators within and outside clusters, the study of regulators related to precursor supply has also been considered in the construction of regulatory networks. The *bkd* cluster encodes a branched α-ketoacid dehydrogenase (BCDH) complex, which catalyzes the production of key intermediates, isobutyryl-CoA and isopentanoyl-CoA [41–44]. These intermediates are critical for the biosynthesis of branched-chain fatty acids (BCFAs), which are essential for the formation of multiple A40926B0 homologs. BkdR acts as a direct transcriptional activator of the *bkd* gene cluster in *Streptomyces roseus*, facilitating the production of these key precursors [45,46]. By protein sequence alignment, we identified its homologous protein ORF6990 (Fig. 5A).

The results revealed that the knockout or overexpression of *bkdR* had no significant impact on strain growth (Fig. 5B and C). However, the knockout of *bkdR* resulted in a 31 % reduction in A40926B0 biosynthesis

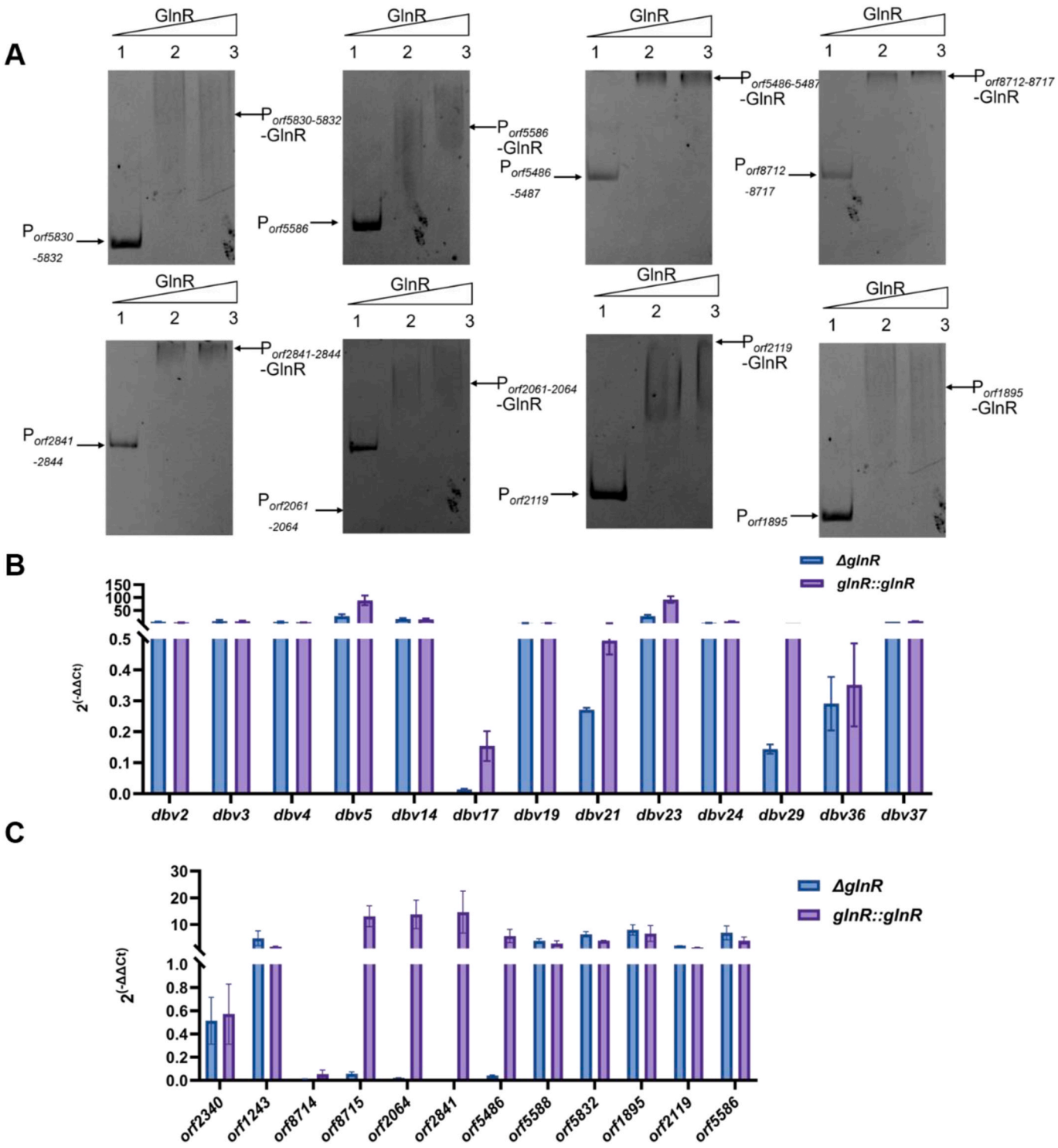

Fig. 4. Identification of regulatory targets of GlnR. (A) Promoter assay for GlnR protein interaction. Lanes 1–3 show EMSA results with 0 μg, 0.05 μg, and 0.1 μg of purified GlnR protein, respectively. (B) Effect of *glnR* deletion on the transcript levels of *dbv* cluster transcriptional units. (n = 3, mean ± SD). (C) Impact of *glnR* deletion on the transcript levels of other secondary metabolism-related transcriptional units. (n = 3, mean ± SD).

to 65 mg/L, whereas the overexpression of *bkdR* increased A40926B0 production by 67 %–159 mg/L compared to the WT (Fig. 5D). qRT-PCR analysis revealed that the knockout of *bkdR* led to a decrease in the transcription levels of genes within both *bkd* clusters, while overexpression of *bkdR* significantly upregulated the expression of these genes (Fig. 5E). EMSA experiments further confirmed that BkdR directly activates the *bkd* cluster, regulating the synthesis of acyl precursors and ultimately influencing A40926B0 biosynthesis (Fig. 5F) (Fig. S9). It has been demonstrated that BkdR acted as a positive regulator, thereby modulating precursor supply and thus positively regulating A40926B0 biosynthesis.

3.5. Reshaping of the regulatory network of A40926B0 biosynthesis

In order to reconstruct the biological regulatory networks of A40926B0, it is necessary to co-express the regulators GlnR, BkdR, and

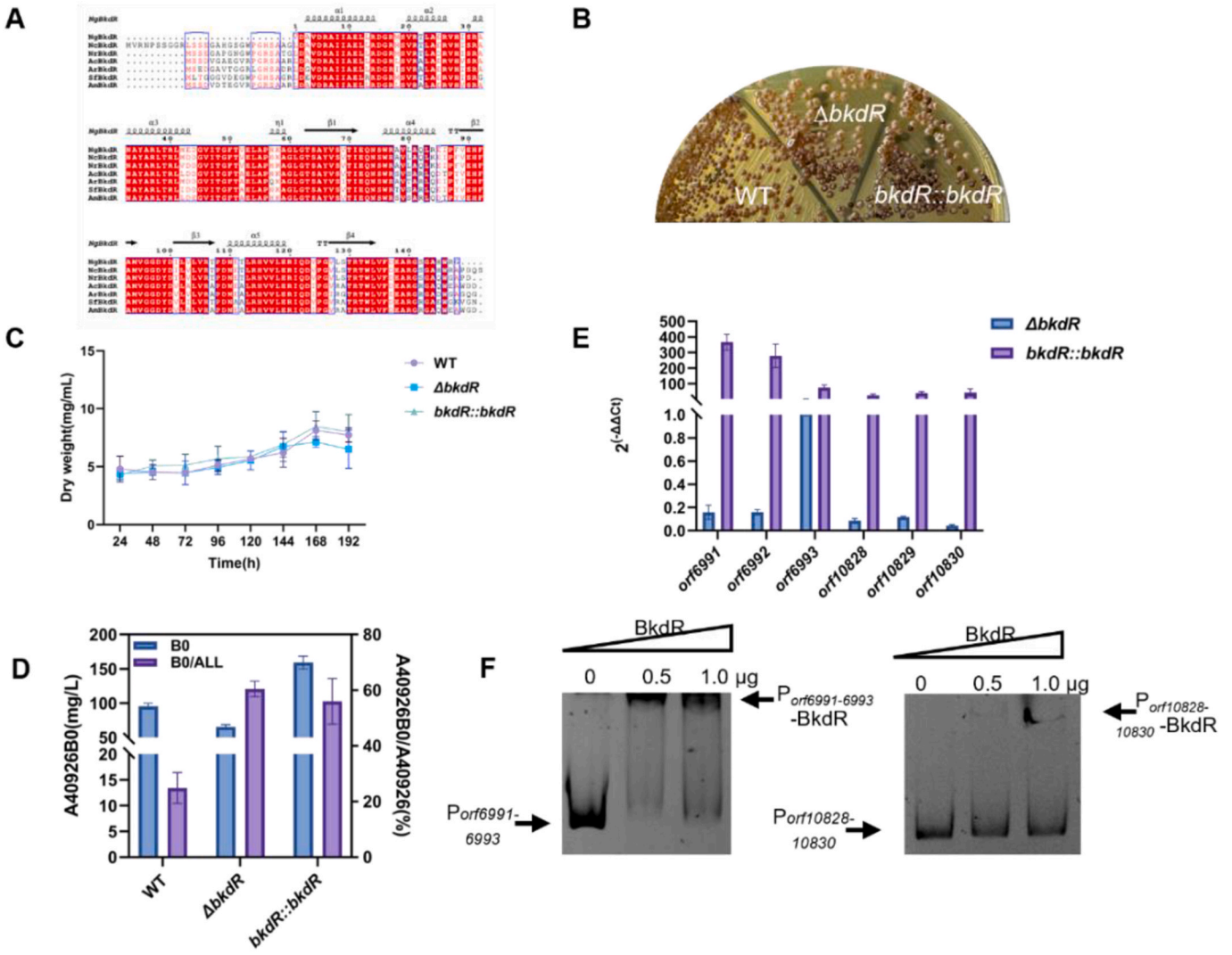

Fig. 5. Functional and regulatory mechanisms of BkdR. (A) Sequence analysis of *bkdR* in *N. gerenzanensis* L70. (B) Effect of *bkdR* deletion on cell growth on solid medium. (C) Effect of *bkdR* deletion on cell growth in liquid medium. (n = 3, mean ± SD). (D) Effect of *bkdR* deletion on A40926B0 production. (n = 3, mean ± SD). (E) Effect of *bkdR* deletion on the transcript levels of each transcriptional unit in the *bkd* cluster. (n = 3, mean ± SD). (F) Binding site probing of BkdR. Lanes 1–3 show EMSA results with 0 μg, 0.05 μg, and 0.1 μg of purified BkdR protein, respectively.

Dbv3, which span the three regulatory dimensions, in a strain in which the *wblA* gene has been knocked out (designated as *OE*) (Fig. 6A). The *OE* strain showed more growth ability in liquid medium. Fermentation results showed that the production of A40926B0 in *OE* was 24 % higher than that of WT, reaching 192 mg/L, and A40926B0 accounted for 65 % of the total homologs, which was 54 % higher than that of WT. Of particular significance was the observation that the B0/B1 ratio of *OE* increased by 92 %, and the total percentage of branched/straight chain homologs increased by 96 %, which resulted in a significant enhancement in the purity of A40926B0. When sodium isobutyrate (a precursor for fatty acid side chain synthesis) was added to the medium at a concentration of 10 mM, the production of A40926B0 increased by 53 % and the total amount of all homologs increased by 83 % (Fig. 6C–E).

Furthermore, EMSA experiments revealed that both GlnR and Dbv3 bind to the P3 (upstream regions of *dbv4*) probe. To investigate the interaction between these two regulators, competitive EMSA experiments were conducted. The results showed that their interaction on P3 was significantly stronger when both proteins were present simultaneously, compared to when they were introduced individually. This suggests that GlnR and Dbv3 can synergistically act on the P3 promoter without competitive inhibition (Fig. 6B).

After identifying the binding sites of each regulatory protein, this study integrated previous findings to propose, for the first time, a three-dimensional regulatory network for A40926B0 biosynthesis, encompassing precursor supply regulation, pleiotropic regulation, and pathway-specific regulation (Fig. 6F). The network was then reconstructed by synthesizing all relevant regulators.

4. Discussion

Advancements in the study of regulatory mechanisms governing antibiotic biosynthesis in actinomycetes have led to the development of various tools to reconstructe known regulatory pathways [21]. WblA, a member of the WhiB-like (Wbl) family of proteins, is a pleiotropic regulator unique to actinomycetes such as *Streptomyces*, *Corynebacterium*, and *Mycobacterium* [47,48]. Recognized as a key transcriptional regulator, WblA is involved in morphological differentiation and development. Typically, WblA functions as a transcriptional repressor; its deficiency promotes the production of several important antibiotics, including the anticancer agent adriamycin and the anti-infective daptomycin, and can even activate latent gene clusters [49]. In some instances, WblA positively regulates the biosynthesis of natural products, such as natamycin and polycyclic tetracosactam [34,50–55]. Despite these insights, experimental evidence directly confirming WblA's

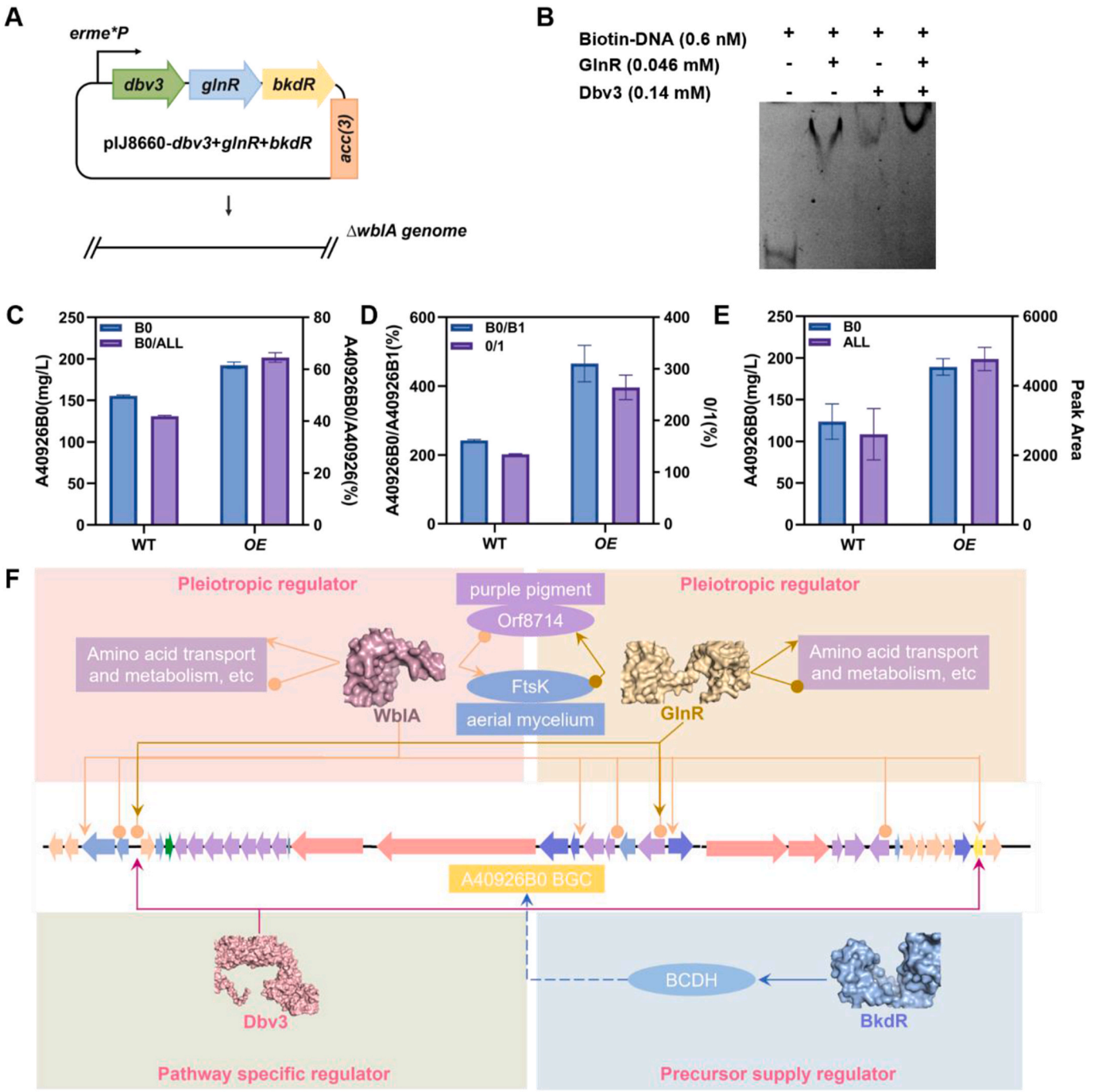

Fig. 6. Reconstruction of the regulatory network for biosynthesis of A40926B0. (A) Diagram illustrating the construction strategy of the overexpression (*OE*) strain. (B) Synergistic regulation of P3 by GlnR and Dbv3. (C) Impact of *OE* on A40926B0 production. (n = 3, mean ± SD). (D) Effect of *OE* on the distribution of A40926 branched homologs and straight-chain homologs. Production of A40926B0/A40926B1 by WT and *OE* strains and the percentage of the total branched-chain homologs (A0 + B0 + C0 + D0) versus straight-chain homologs (A1 + B1 + C1 + D1) (n = 3, mean ± SD). (E) Effect of continuous supplementation with 10 mM sodium isobutyrate in the YS medium on A40926B0 production in the reconstituted *OE* strain. (n = 3, mean ± SD). (F) Schematic representation of the regulatory network involved in A40926B0 biosynthesis. Arrows (→) indicate positive regulation, while circles (−o) represent negative regulation. Solid lines represent direct regulation, and dashed lines indicate indirect regulation.

binding to specific promoter sequences is still lacking, leaving its exact regulatory targets and mechanisms unclear [56].

To investigate its regulatory role, we constructed both knockout and overexpression strains of *wblA*. The knockout of *wblA* resulted in hindered growth, with the strain failing to produce aerial mycelium properly. Notably, violet pigment production was significantly increased, and the cells became shorter and unbranched, indicating severe impairment in aerial mycelium development. WblA negatively regulated the biosynthesis of A40926B0. In addition, WblA negatively regulated A40926B0 biosynthesis. *wblA* knockout decreased the expression of key genes in the A40926B0 biosynthesis pathway, but up-regulation of other genes related to secondary metabolism contributed to the increase in A40926B0 production. The GUS reporter system further confirmed that WblA directly interacts with multiple transcriptional units within the *dbv* gene cluster, including genes encoding regulatory proteins, NRPS synthetases and modifying enzymes. Additionally, WblA was found to

indirectly influence A40926B0 biosynthesis by interacting with proteins involved in amino acid and fatty acid metabolism.

Dbv3 is another critical regulator within the A40926B0 biosynthetic gene cluster, with overexpression of Dbv3 having the most pronounced effect on A40926B0 biosynthesis [18], whereas the biosynthesis of all homologs is inhibited following the knockout of *dbv3*. The Dbv3 binding site has been localized in the upstream region of *dbv4* and *dbv36-37*. To identify potential regulators of *dbv3*, this study employed a top-down (protein-to-DNA) multi-omics approach [24,25,57]. Using biotin-labeled P2 (upstream regions of *dbv3*) as bait, we isolated and identified GlnR from *N. gerenzanensis* L70. EMSA experiments confirmed that GlnR binds to the *dbv3* promoter.

GlnR is a global transcriptional regulator involved in nitrogen metabolism. Under nitrogen-limiting conditions, it activates the majority of nitrogen assimilation genes in *Streptomyces* [57–59]. In *Bacillus subtilis*, GlnR acts as a secondary regulator, repressing nitrogen assimilation genes [60], while in *Lactobacillus*, it negatively regulates glutamate-dependent acid tolerance [61]. GlnR directly and positively regulates several key regulatory genes within the *dbv* gene cluster, including *dbv3*, *dbv4*, and *dbv22*. GlnR also influences aerial mycelium growth and pigment synthesis, which are vital for A40926B0 biosynthesis. qRT-PCR experiments confirmed that overexpression of *glnR* enhanced the transcription of genes within the *dbv* cluster, as well as genes involved in amino acid metabolism, thereby promoting A40926B0 production. In conclusion, the identification of GlnR as a key regulator enhances the understanding of the complex regulatory network controlling A40926B0 biosynthesis.

Isobutyryl-CoA and isovaleryl-CoA, essential precursors of BCFAs involved in A40926B0 biosynthesis, are derived from the catabolism of branched-chain amino acids. The BCDH complex, which catalyzes these precursors, plays a crucial role in BCFA biosynthesis [62,63]. BkdR is a regulator of the BCDH gene cluster, and its deletion in *Streptomyces albidus* B4 was found to enhance the supply of malonyl- and methylmalonyl-coenzyme A precursors [46]. In *Streptomyces azureus*, the BkdR protein acts as a negative regulator of the BCDH gene cluster [45]. This study observed that the knockout of *bkdR* led to a 31 % reduction in A40926B0 biosynthesis, while overexpression of *bkdR* significantly increased the production by 67 %. EMSA experiments confirmed that BkdR positively regulated the *bkd* gene cluster, modulating the synthesis of acyl precursors, which in turn influences A40926B0 biosynthesis.

In summary, this study integrated the roles of key regulators—WblA, GlnR, BkdR, and Dbv3—to reconstruct the regulatory network controlling A40926B0 biosynthesis. Co-expression of GlnR, BkdR, and Dbv3 resulted in a 24 % increase in A40926B0 production compared to the WT, along with a significant improvement in product purity, with a 92 % increase in the B0/B1 ratio. Furthermore, supplementation with sodium isobutyrate, a precursor for fatty acid side-chain synthesis, enhanced A40926B0 production by 53 % and increased the total amount of homologs by 83 %.

5. Conclusion

New insights into the regulatory mechanisms governing A40926B0 biosynthesis in *N. gerenzanensis* L70 have been provided. The construction of a multidimensional model of the A40926B0 biosynthetic regulatory network has been achieved by elucidating the roles of key regulatory factors. WblA is proposed to play a central role in regulating secondary metabolism, laying the groundwork for further exploration into its broader regulatory network. For the first time, the pathway-specific regulatory target of Dbv3 in A40926B0 biosynthesis is confirmed, revealing a cascade regulation involving Dbv3 and Dbv4 within the gene cluster. This finding adds a new layer to our understanding of how specific pathways are governed at the transcriptional level. In addition to Dbv3 and Dbv4, GlnR, identified through a bottom-up (DNA-to-protein) regulator mining strategy, has emerged as a critical multipotent regulator. Furthermore, BkdR, a regulator involved in precursor synthesis, has been identified as an essential component of the overall regulatory network, linking precursor supply to secondary metabolism. By reconstructing the regulatory network through the co-expression of GlnR, BkdR, and Dbv3 in a WblA knockout strain, we achieved a 92 % improvement in its purity.

The regulatory network model we propose encompasses three key dimensions: precursor supply regulation, multipotent regulation, and pathway-specific regulation. This model not only advances our understanding of the complex regulatory network controlling A40926B0 biosynthesis but also offers a valuable framework for future research. Such insights can be applied to improve the biosynthesis of other natural products, with significant implications for the production of antibiotics and other bioactive compounds.

CRediT authorship contribution statement

Yan-Qiu Liu: Writing – original draft, Methodology, Formal analysis, Data curation. **Yi-Lei Zheng:** Supervision, Software. **Ye Xu:** Supervision, Project administration. **Xue-Yan Liu:** Formal analysis. **Tian-Yu Xia:** Supervision, Methodology. **Qing-Wei Zhao:** Investigation. **Yong-Quan Li:** Writing – review & editing, Resources, Funding acquisition, Conceptualization.

Data availability

The transcriptome data are available in the SRA under accession number PRJNA1204282 (https://www.ncbi.nlm.nih.gov/sra). Post-treatment expression data (FPKM values) are available in GEO under accession number GSE289867 (https://www.ncbi.nlm.nih.gov/geo/).

Declaration of competing interest

The authors declare that they have no known competing financial interests or personal relationships that could have appeared to influence the work reported in this paper.

Acknowledgments

We thank all the people who participated in this work. We would like to thank Xiao-Dan Wu in the Analysis Center of Agrobiology and Environmental Sciences for high-resolution proteomic analysis assistance, GENEWIZ for transcriptome analysis assistance. We thank Gui-Zhen Zhu in the Center of Cryo-Electron Microscopy (CCEM), Zhejiang University, for their technical assistance with SEM.

This work was supported by the National Natural Science Foundation of China (grant number 32170057).

Appendix A. Supplementary data

Supplementary data to this article can be found online at https://doi.org/10.1016/j.synbio.2025.03.012.

References

[1] Lopez S, Hackbarth C, Romanò G, Trias J, Jabes D, Goldstein BP. *In vitro* antistaphylococcal activity of dalbavancin, a novel glycopeptide. J Antimicrob Chemother 2005;55(Suppl 2):ii21–24. https://doi.org/10.1093/jac/dki007.

[2] Goldstein BP, Draghi DC, Sheehan DJ, Hogan P, Sahm DF. Bactericidal activity and resistance development profiling of dalbavancin. Antimicrob Agents Chemother 2007;51:1150–4. https://doi.org/10.1128/aac.00620-06.

[3] Bailey J, Summers KM. Dalbavancin: a new lipoglycopeptide antibiotic. Am J Health Syst Pharm 2008;65:599–610. https://doi.org/10.2146/ajhp070255.

[4] Cercenado E. Antimicrobial spectrum of dalbavancin. Mechanism of action and *in vitro* activity against Gram-positive microorganisms. Enferm Infecc Microbiol Clín 2017;35(Suppl 1):9–14. https://doi.org/10.1016/s0213-005x(17)30029-0.

[5] Werth BJ, Ashford NK, Penewit K, Waalkes A, Holmes EA, Ross DH, et al. Dalbavancin exposure *in vitro* selects for dalbavancin-non-susceptible and

vancomycin-intermediate strains of methicillin-resistant *Staphylococcus aureus*. Clin Microbiol Infect 2021;27:910.e1–8. https://doi.org/10.1016/j.cmi.2020.08.025.
[6] Huang V, Cheung CM, Kaatz GW, Rybak MJ. Evaluation of dalbavancin, tigecycline, minocycline, tetracycline, teicoplanin and vancomycin against community-associated and multidrug-resistant hospital-associated meticillin-resistant *Staphylococcus aureus*. Int J Antimicrob Agents 2010;35:25–9. https://doi.org/10.1016/j.ijantimicag.2009.08.020.
[7] Huband MD, Castanheira M, Farrell DJ, Flamm RK, Jones RN, Sader HS, et al. *In vitro* activity of dalbavancin against multidrug-resistant *Staphylococcus aureus* and *streptococci* from patients with documented infections in Europe and surrounding regions (2011-2013). Int J Antimicrob Agents 2016;47:495–9. https://doi.org/10.1016/j.ijantimicag.2016.04.009.
[8] Koulenti D, Xu E, Mok IYS, Song A, Karageorgopoulos DE, Armaganidis A, et al. Novel antibiotics for multidrug-resistant Gram-positive microorganisms. Microorganisms 2019;7:270. https://doi.org/10.3390/microorganisms7080270.
[9] Gatti M, Andreoni M, Pea F, Viale P. Real-world use of dalbavancin in the era of empowerment of outpatient antimicrobial treatment: a careful appraisal beyond approved indications focusing on unmet clinical needs. Drug Des Dev Ther 2021;15:3349–78. https://doi.org/10.2147/dddt.s313756.
[10] Van Bambeke F, Van Laethem Y, Courvalin P, Tulkens PM. Glycopeptide antibiotics: from conventional molecules to new derivatives. Drugs 2004;64:913–36. https://doi.org/10.2165/00003495-200464090-00001.
[11] Dorr MB, Jabes D, Cavaleri M, Dowell J, Mosconi G, Malabarba A, et al. Human pharmacokinetics and rationale for once-weekly dosing of dalbavancin, a semi-synthetic glycopeptide. J Antimicrob Chemother 2005;55(Suppl 2):ii25–30. https://doi.org/10/cq9g5d.
[12] Alt S, Bernasconi A, Sosio M, Brunati C, Donadio S, Maffioli SI. Toward single-peak dalbavancin analogs through biology and chemistry. ACS Chem Biol 2019;14:356–60. https://doi.org/10.1021/acschembio.9b00050.
[13] Sosio M, Stinchi S, Beltrametti F, Lazzarini A, Donadio S. The gene cluster for the biosynthesis of the glycopeptide antibiotic A40926 by *nonomuraea* species. Chem Biol 2003;10:541–9. https://doi.org/10/db4mzn.
[14] Gunnarsson N, Bruheim P, Nielsen J. Production of the glycopeptide antibiotic A40926 by *Nonomuraea sp.* ATCC 39727: influence of medium composition in batch fermentation. J Ind Microbiol Biotechnol 2003;30:150–6. https://doi.org/10/fftxdp.
[15] Beltrametti F, Jovetic S, Feroggio M, Gastaldo L, Selva E, Marinelli F. Valine influences production and complex composition of glycopeptide antibiotic A40926 in fermentations of *Nonomuraea sp.* ATCC 39727. J Antibiot (Tokyo) 2004;57:37–44. https://doi.org/10/g8xbfn.
[16] Jovetic S, Feroggio M, Marinelli F, Lancini G. Factors influencing cell fatty acid composition and A40926 antibiotic complex production in *Nonomuraea sp.* ATCC 39727. J Ind Microbiol Biotechnol 2008;35:1131–8. https://doi.org/10/crcn6q.
[17] Dong H, Yue X, Yan B, Gao W, Wang S, Li Y. Improved A40926 production from *Nonomuraea gerenzanensis* using the promoter engineering and the co-expression of crucial genes. J Biotechnol 2020;324:28–33. https://doi.org/10/gs2zkz.
[18] Xia T-Y, Chen X-A, Liu Y-Q, Scharf DH, Zhao Q-W, Li Y-Q. Redirection of acyl donor metabolic flux for lipopeptide A40926B0 biosynthesis. Microb Biotechnol 2022;15:1852–66. https://doi.org/10/gspwtm.
[19] Dietrich JA, Shis DL, Alikhani A, Keasling JD. Transcription factor-based screens and synthetic selections for microbial small-molecule biosynthesis. ACS Synth Biol 2013;2:47–58. https://doi.org/10/f4v9nm.
[20] Porokhin V, Amin SA, Nicks TB, Gopinarayanan VE, Nair NU, Hassoun S. Analysis of metabolic network disruption in engineered microbial hosts due to enzyme promiscuity. Metab Eng Commun 2021;12:e00170. https://doi.org/10/grk2mz.
[21] Zobel S, Kumpfmüller J, Süssmuth RD, Schweder T. *Bacillus subtilis* as heterologous host for the secretory production of the non-ribosomal cyclodepsipeptide enniatin. Appl Microbiol Biotechnol 2015;99:681–91. https://doi.org/10.1007/s00253-014-6199-0.
[22] Xia H, Li X, Li Z, Zhan X, Mao X, Li Y. The application of regulatory cascades in *Streptomyces*: yield enhancement and metabolite mining. Front Microbiol 2020;11:406. https://doi.org/10/g8xbfm.
[23] Zhu Y, Zhang P, Zhang J, Wang J, Lu Y, Pang X. Impact on multiple antibiotic pathways reveals MtrA as a master regulator of antibiotic production in *Streptomyces spp.* and potentially in other *Actinobacteria*. Appl Environ Microbiol 2020;86:e01201. 20, https://doi.org/10/g8xbd2.
[24] Xie H, Ruan J-Y, Bu Q-T, Li Y-P, Su Y-T, Zhao Q-W, et al. Transcriptional regulation of the fidaxomicin gene cluster and cellular development in *Actinoplanes deccanensis* YP-1 by the pleiotropic regulator MtrA. Microbiol Spectr 2023;11:e0270223. https://doi.org/10/g8xbdx.
[25] Mao X-M, Luo S, Zhou R-C, Wang F, Yu P, Sun N, et al. Transcriptional regulation of the daptomycin gene cluster in *Streptomyces roseosporus* by an autoregulator, AtrA. J Biol Chem 2015;290:7992–8001. https://doi.org/10/f66jj4.
[26] Chen L, Lu Y, Chen J, Zhang W, Shu D, Qin Z, et al. Characterization of a negative regulator AveI for avermectin biosynthesis in *Streptomyces avermitilis* NRRL8165. Appl Microbiol Biotechnol 2008;80:277–86. https://doi.org/10/dhbwqt.
[27] Cloney R. Gene regulation: a gene-centric analysis of transcriptional cascades. Nat Rev Genet 2016;17:193. https://doi.org/10/g8xbdw.
[28] Alduina R, Lo Piccolo L, D'Alia D, Ferraro C, Gunnarsson N, Donadio S, et al. Phosphate-controlled regulator for t36he biosynthesis of the dalbavancin precursor A40926. J Bacteriol 2007;189:8120–9. https://doi.org/10/cxbwsm.
[29] Alduina R, Tocchetti A, Costa S, Ferraro C, Cancemi P, Sosio M, et al. A Two-Component regulatory system with opposite effects on glycopeptide antibiotic biosynthesis and resistance. Sci Rep 2020;10:6200. https://doi.org/10/g8xbfj.
[30] Lo Grasso L, Maffioli S, Sosio M, Bibb M, Puglia AM, Alduina R. Two master switch regulators trigger A40926 biosynthesis in *Nonomuraea* sp. strain ATCC 39727. J Bacteriol 2015;197:2536–44. https://doi.org/10/g8xbdz.
[31] Rube HT, Rastogi C, Feng S, Kribelbauer JF, Li A, Becerra B, et al. Prediction of protein-ligand binding affinity from sequencing data with interpretable machine learning. Nat Biotechnol 2022;40:1520–7. https://doi.org/10.1038/s41587-022-01307-0.
[32] Xie VC, Styles MJ, Dickinson BC. Methods for the directed evolution of biomolecular interactions. Trends Biochem Sci 2022;47:403–16. https://doi.org/10.1016/j.tibs.2022.01.001.
[33] Li Y-P, Yu P, Li J-F, Tang Y-L, Bu Q-T, Mao X-M, et al. FadR1, a pathway-specific activator of fidaxomicin biosynthesis in *Actinoplanes deccanensis* Yp-1. Appl Microbiol Biotechnol 2019;103:7583–96. https://doi.org/10.1007/s00253-019-09949-y.
[34] Huang X, Ma T, Tian J, Shen L, Zuo H, Hu C, et al. *wblA*, a pleiotropic regulatory gene modulating morphogenesis and daptomycin production in *Streptomyces roseosporus*. J Appl Microbiol 2017;123:669–77. https://doi.org/10/ghb42m.
[35] Wang L, Lutkenhaus J. FtsK is an essential cell division protein that is localized to the septum and induced as part of the SOS response. Mol Microbiol 1998;29:731–40. https://doi.org/10/cz36sq.
[36] Aussel L, Barre FX, Aroyo M, Stasiak A, Stasiak AZ, Sherratt D. FtsK Is a DNA motor protein that activates chromosome dimer resolution by switching the catalytic state of the XerC and XerD recombinases. Cell 2002;108:195–205. https://doi.org/10/cfppk6.
[37] Mishra S, Misra HS, Kota S. FtsK, a DNA motor protein, coordinates the genome segregation and early cell division processes in *Deinococcus radiodurans*. mBio 2022;13:e0174222. https://doi.org/10/gq5bhr.
[38] Yan L, Zhang Q, Virolle M-J, Xu D. In conditions of over-expression, WblI, a WhiB-like transcriptional regulator, has a positive impact on the weak antibiotic production of *Streptomyces lividans* TK24. PLoS One 2017;12:e0174781. https://doi.org/10/gqn535.
[39] Zhu Y, Wang X, Zhang J, Ni X, Zhang X, Tao M, et al. The regulatory gene *wblA* is a target of the orphan response regulator OrrA in *Streptomyces coelicolor*. Environ Microbiol 2022;24:3081–96. https://doi.org/10/gqn53t.
[40] He J-M, Zhu H, Zheng G-S, Liu P-P, Wang J, Zhao G-P, et al. Direct involvement of the master nitrogen metabolism regulator GlnR in antibiotic biosynthesis in *Streptomyces*. J Biol Chem 2016;291:26443–54. https://doi.org/10/f9k4rn.
[41] Ward DE, Ross RP, van der Weijden CC, Snoep JL, Claiborne A. Catabolism of branched-chain alpha-keto acids in *Enterococcus faecalis*: the *bkd* gene cluster, enzymes, and metabolic route. J Bacteriol 1999;181:5433–42. https://doi.org/10/gqms6b.
[42] Pulsawat N, Kitani S, Kinoshita H, Lee CK, Nihira T. Identification of the *bkdAB* gene cluster, a plausible source of the starter-unit for virginiamycin M production in *Streptomyces virginiae*. Arch Microbiol 2007;187:459–66. https://doi.org/10/dw57q8.
[43] Bode HB, Ring MW, Schwär G, Altmeyer MO, Kegler C, Jose IR, et al. Identification of additional players in the alternative biosynthesis pathway to isovaleryl-CoA in the myxobacterium *Myxococcus xanthus*. ChemBioChem 2009;10:128–40. https://doi.org/10/c5f85p.
[44] Sprusansky O, Stirrett K, Skinner D, Denoya C, Westpheling J. The *bkdR* gene of *Streptomyces coelicolor* is required for morphogenesis and antibiotic production and encodes a transcriptional regulator of a branched-chain amino acid dehydrogenase complex. J Bacteriol 2005;187:664–71. https://doi.org/10/fg2js3.
[45] Luo S, Chen X-A, Mao X-M, Li Y-Q. Regulatory and biosynthetic effects of the *bkd* gene clusters on the production of daptomycin and its analogs A21978C1-3. J Ind Microbiol Biotechnol 2018;45:271–9. https://doi.org/10/gc72ds.
[46] Wang W, Tang H, Cui X, Wei W, Wu J, Ye B-C. Engineering of a TetR family transcriptional regulator BkdR enhances heterologous spinosad production in *Streptomyces albus* B4 chassis. Appl Environ Microbiol 2024;90:e0083824. https://doi.org/10/g8xbd5.
[47] Bush MJ. The *actinobacterial* WhiB-like (Wbl) family of transcription factors. Mol Microbiol 2018;110:663–76. https://doi.org/10/gfjhbr.
[48] Burkovski A. Ammonium assimilation and nitrogen control in *Corynebacterium glutamicum* and its relatives: an example for new regulatory mechanisms in actinomycetes. FEMS Microbiol Rev 2003;27:617–28. https://doi.org/10/dnwqht.
[49] Makitrynskyy R, Tsypik O, Nuzzo D, Paululat T, Zechel DL, Bechthold A. Secondary nucleotide messenger c-di-GMP exerts a global control on natural product biosynthesis in *streptomycetes*. Nucleic Acids Res 2020;48:1583–98. https://doi.org/10/ggh82b.
[50] Kang S-H, Huang J, Lee H-N, Hur Y-A, Cohen SN, Kim E-S. Interspecies DNA microarray analysis identifies WblA as a pleiotropic down-regulator of antibiotic biosynthesis in *Streptomyces*. J Bacteriol 2007;189:4315–9. https://doi.org/10/dxqw6m.
[51] Yu P, Liu S-P, Bu Q-T, Zhou Z-X, Zhu Z-H, Huang F-L, et al. WblAch, a pivotal activator of natamycin biosynthesis and morphological differentiation in *Streptomyces chattanoogensis* L10, is positively regulated by AdpAch. Appl Environ Microbiol 2014;80:6879–87. https://doi.org/10/f6np2g.
[52] Huang H, Hou L, Li H, Qiu Y, Ju J, Li W. Activation of a plasmid-situated type III PKS gene cluster by deletion of a *wbl* gene in deepsea-derived *Streptomyces somaliensis* SCSIO ZH66. Microb Cell Fact 2016;15:116. https://doi.org/10/gqn538.
[53] Bu X-L, Weng J-Y, He-Lin Yu, Xu M-J, Xu J. Three transcriptional regulators positively regulate the biosynthesis of polycyclic tetramate macrolactams in *Streptomyces xiamenensis* 318. Appl Microbiol Biotechnol 2020;104:701–11. https://doi.org/10/gqn532.

[54] Zhang F, Gao D, Lin J, Zhu M, Zhuang Z, Duan Y, et al. Construction of inducible genetic switch for the global regulator WblA to sustain both overproduction of tiancimycins and on-demand sporulation in *Streptomyces* sp. CB03234. ACS Synth Biol 2020;9:1460–7. https://doi.org/10/gqn53z.
[55] Zhang W, Mou M, Hu W, Lu M, Zhang H, Zhang H, et al. MOINER: a novel multiomics early integration framework for biomedical classification and biomarker discovery. J Chem Inf Model 2024;64:2720–32. https://doi.org/10/g8xbd3.
[56] Nah H-J, Park J, Choi S, Kim E-S. WblA, a global regulator of antibiotic biosynthesis in *Streptomyces*. J Ind Microbiol Biotechnol 2021;48:kuab007. https://doi.org/10/gkcgjt.
[57] Zhu Y, Wang J, Su W, Lu T, Li A, Pang X. Effects of dual deletion of *glnR* and *mtrA* on expression of nitrogen metabolism genes in *Streptomyces venezuelae*. Microb Biotechnol 2022;15:1795–810. https://doi.org/10/gsx5bw.
[58] Wang R, Mast Y, Wang J, Zhang W, Zhao G, Wohlleben W, et al. Identification of two-component system AfsQ1/Q2 regulon and its cross-regulation with GlnR in *Streptomyces coelicolor*. Mol Microbiol 2013;87:30–48. https://doi.org/10/g8xbd6.
[59] Fernandes G de C, Hauf K, Sant'Anna FH, Forchhammer K, Passaglia LMP. Glutamine synthetase stabilizes the binding of GlnR to nitrogen fixation gene operators. FEBS J 2017;284:903–18. https://doi.org/10/g8xbfb.
[60] Gutowski JC, Schreier HJ. Interaction of the Bacillus subtilis *glnRA* repressor with operator and promoter sequences *in vivo*. J Bacteriol 1992;174:671–81. https://doi.org/10/g8xbd8.
[61] Gong L, Ren C, Xu Y. GlnR negatively regulates glutamate-dependent acid resistance in *Lactobacillus brevis*. Appl Environ Microbiol 2020;86:e02615. 19, https://doi.org/10/g8xbd7.
[62] Stirrett K, Denoya C, Westpheling J. Branched-chain amino acid catabolism provides precursors for the Type II polyketide antibiotic, actinorhodin, via pathways that are nutrient dependent. J Ind Microbiol Biotechnol 2009;36:129–37. https://doi.org/10/b6s8z6.
[63] Madhusudhan KT, Lorenz D, Sokatch JR. The *bkdR* gene of *Pseudomonas putida* is required for expression of the *bkd* operon and encodes a protein related to Lrp of *Escherichia coli*. J Bacteriol 1993;175:3934–40. https://doi.org/10/g8xbd4.